EMI from Apertures at Enclosure Cavity Mode Resonances

M. Li, Y. Ji, S. Radu, J. Nuebel*, W. Cui
J.L.Drewniak, T.H.Hubing, T.P.VanDoren

Electromagnetic Compatibility Laboratory
Department of Electrical Engineering
University of Missouri–Rolla
Rolla, MO 65409-0040

*Electromagnetic Compatibility Group
Sun Microsystems, Inc.
2550 Garcia Avenue
Mountain View, CA 94043-1100

abstract: EMI from slots and apertures resulting from coupling of interior sources through enclosure cavity modes in a Sun S-1000 workstation was investigated. The excitation of a specially designed rectangular enclosure with a slot was also studied experimentally and with finite-difference time-domain (FDTD) simulations. The radiated power results for both the S-1000 and simple rectangular enclosure indicate that radiation at cavity mode resonance frequencies through slots and apertures can be as significant as at aperture or slot resonances. A decrease of the radiation through the slots and apertures can be achieved by employing a lossy material in the enclosure.

I. Introduction

The integrity of shielding enclosures is compromised by slots and apertures for heat dissipation, CD-ROMs, I/O cable penetration, and plate-covered unused connector holes, among other possibilities. Radiation from slots and apertures in conducting enclosures excited by interior sources, is of great concern in meeting FCC radiated EMI limits. Energy coupling between cavity modes and a slot has previously been studied numerically [1], [2], while experimental investigations are limited.

It is well known that an appropriately excited slot in a conductor radiates with peaks at frequencies where the slot is of integer half-wavelength dimensions [3]. A simple maxim in enclosure design is to restrict slot dimensions below a half-wave length. As clock frequencies increase and enclosure dimensions become electrically large, this is achieved with gasketing and/or strategically placed conducting fingers. Results presented in this paper indicate that cavity mode resonances can result in significant radiation through non-resonant length slots. An S-1000 server was investigated by two-port S-parameter measurements. The radiation through slots and apertures at cavity mode resonances was significant. The locations and geometry of interior sources were important for the excitation of cavity mode resonances [4].

A simple rectangular enclosure with one thin slot fed with a wire probe was investigated experimentally and with FDTD simulations. With appropriate modeling of the essential features such as the source, load, and loss, the FDTD simulated results agreed with the measurements. The results indicate that the radiation at cavity mode resonances is as significant as the radiation at the resonances due to the slot. Further, interaction between the cavity and slot resulted in resonances that were associated with neither alone. The radiation at these resonances can be significant.

The effect of a dielectric lossy material in reducing EMI was investigated in the S-1000. The results show that the lossy material can be effective. However, the location of the lossy material and the EMI noise source at the PCB level is important to this effect.

II. Experiments and FDTD simulations

A Sun S-1000 enclosure with all potential slots and apertures determined from radiated EMI measurements on a functioning production design is shown in Figure 1. The potential slots and apertures (numbered in Figure 1) are essentially located on front and rear panels. The hole pattern on each side for airflow contributed negligibly to the measured EMI. The enclosure was partitioned into front and rear portions by a center plane. The power supply was located in the front portion. Two-port S-parameters were measured in a semianechoic chamber, where a source in the enclosure under test was connected to Port 1 of a Wiltron 37247A network analyzer, and a horn antenna as the re-

0-7803-4140-6/97/$10.00

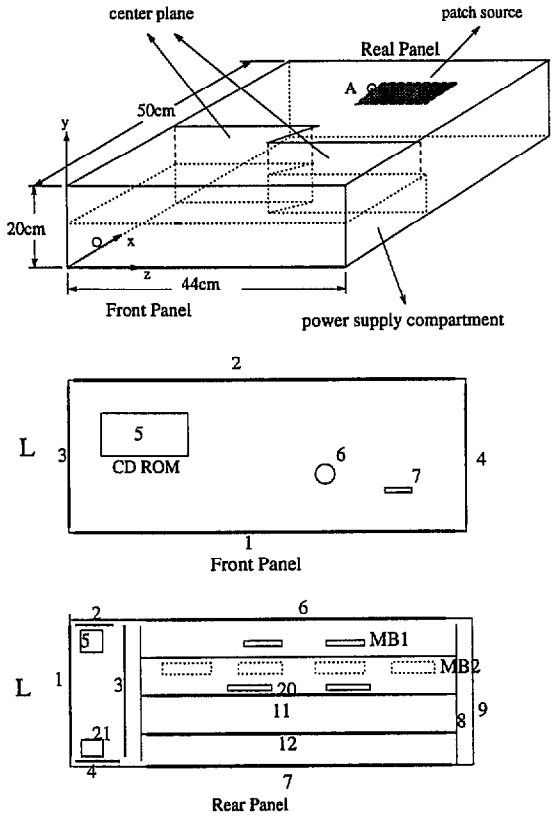

Figure 1. Configuration of the Sun S-1000 workstation enclosure.

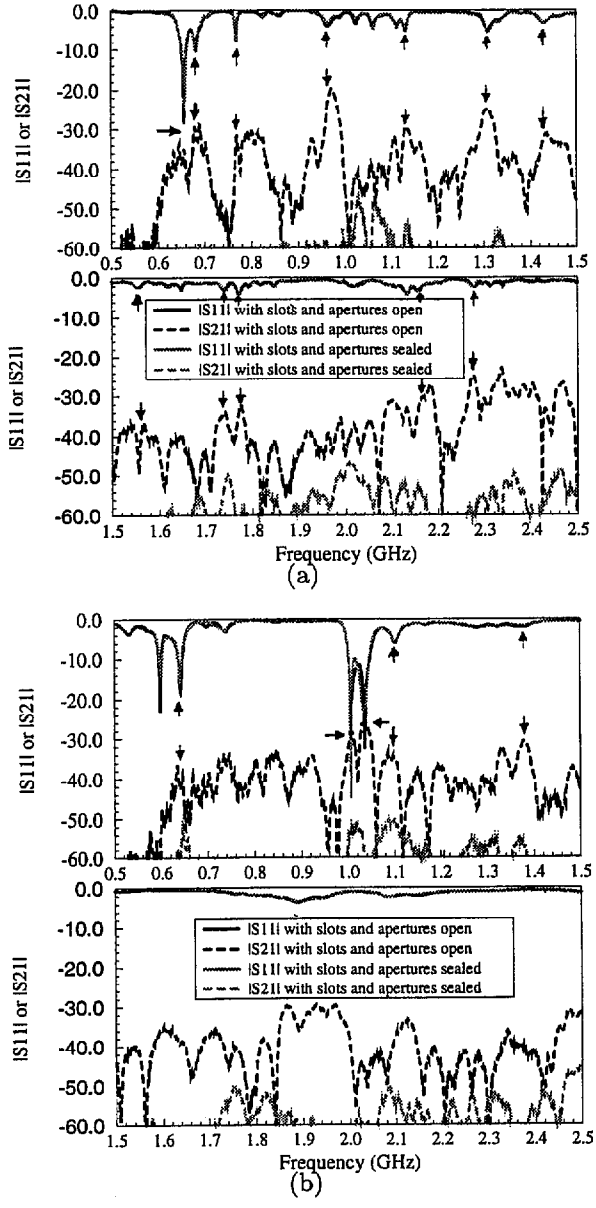

Figure 2. Measured $|S_{11}|$ and $|S_{21}|$ of the S-1000 excited by a patch source at Point A, (a) without the interior electronics, and (b) with the interior electronics.

ceiver was connected to Port 2 of the network analyzer. Far field measurements were made since the distance between the device under test and the receiving antenna was 3 m. The network analyzer was placed outside the semianechoic room to measure the reflection coefficient $|S_{11}|$. The transmission coefficient $|S_{21}|$, which is related to the radiated power was also measured. The antenna factor of the receiving horn was not included in the calibration procedure, and the $|S_{21}|$ results were only relative measurements of the effect of slots and apertures from the background measurements (without slots and apertures).

Measurements were made on the S-1000 without and with all the actual electronics present (unpowered). For the situation with the electronics, one motherboard with a single CPU module was in the back portion, and a CD ROM, disk drives, and controller card were in the front portion. The power supply unit was contained within its own shielding enclosure, and was present in all measurements. A source fed from the network analyzer was positioned in the rear portion of the cavity. A patch source was located at Point A, approximately the size and position of a heat sink on the CPU module. This heat sink was determined from the production hardware through extensive modification and testing to be the primary coupling path of CPU harmonics radiated through apertures. For the situation without the interior electronics, the $|S_{11}|$ and $|S_{21}|$ measurements with and without slots and apertures (background) are shown in Figure 2 (a). The measurements with the electronics are shown in Figure 2 (b). There were no significant differences in $|S_{11}|$ for the situations with and without slots and apertures, independent of whether the enclosure was empty or filled with electronics, indicating that the $|S_{11}|$ resonances were cavity mode resonances. The motherboard employed entire planes for ground and power, that effectively partitioned the rear compartment horizontally. The shift in

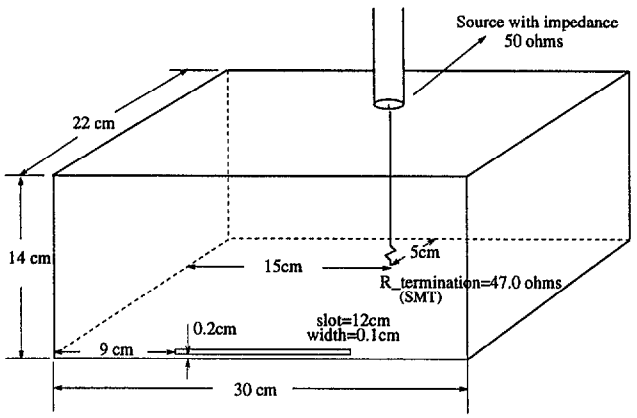

Figure 3. The geometry of the specially designed rectangular enclosure with a single slot.

the resonance frequencies as a result is apparent from Figure 2 (a) and (b).

$|S_{21}|$ generally increased more than 20 dB on average when the slots and apertures were open. For the situation without the electronics, the $|S_{21}|$ resonances at 0.65 GHz, 0.68 GHz, 0.77 GHz, 0.96 GHz, 1.31 GHz, 1.43 GHz, 1.78 GHz, 2.27 GHz, 2.33 GHz, etc., shown by the arrows in Figure 2 (a), were related to the cavity modes from the comparison of $|S_{11}|$ and $|S_{21}|$, which showed that cavity modes were important for exciting slots and apertures. For the situation with the electronics, the resonances on S_{21} at 0.65 GHz, 0.74 GHz, 1.01 GHz, 1.04 GHz, 1.10 GHz, 1.38 GHz, etc., shown by the arrows in Figure 2 (b) were associated with cavity modes. The interior electronics changed $|S_{11}|$ and $|S_{21}|$ significantly, but the effect and mechanism are not well understood and require further study. The conducting planes on the PCB further partitioned the rear compartment. Further, the losses on the board tended to smooth resonances. There were some $|S_{21}|$ resonances which did not correspond to any $|S_{11}|$ resonances. The reason may be that the $|S_{11}|$ was determined by the cavity mode resonances of the rear portion since the exciting source was in the rear portion, while the radiation included the cavity mode resonances of the front portion, which was excited by the slots and apertures in the center plane [5].

A specially designed rectangular enclosure shown in Figure 3 was studied for the excitation of cavity modes and slot modes in a simple situation. The cavity was constructed of 5 pieces of 0.635 cm thick aluminum, and one plate of 0.05 cm thick aluminum for the face containing the slot. A slot of width $w_s = 0.1$ cm ($\frac{w_s}{\delta y} = 0.2$) and length of 12 cm was located 0.25 $cm = \frac{1}{2}\delta y$ from the center of the slot to the bottom edge, where δy is the FDTD mesh dimension along the y-axis. The inside dimensions of the enclosure were 22 $cm \times 14$ $cm \times 30$ cm. One-inch copper tape with conductive adhesive was used to electromagnetically seal the seams. The cavity was fed with a 50 Ω coaxial cable probe through a type-N bulkhead connector, which was peripherally bonded to the cavity. The center conductor of the probe was extended to span the width of the cavity with a 0.16 cm diameter wire, and terminated on the opposite cavity wall with a 1206 package size surface-mount (SMT) 47 Ω resistor stood on end and soldered to a $1.5'' \times 1.5''$ square of conductive adhesive copper tape. The feed probe was located at $x = 17$ cm, $y = 14$ cm, and $z = 15$ cm. The measured real power delivered by the source normalized to the source voltage was calculated from the reflection coefficient as

$$P = \frac{1}{8Z_0}(1 - |S_{11}|^2). \tag{1}$$

A cell size of 1.0 $cm \times 0.5$ $cm \times 1.0$ cm was employed in the FDTD simulations, where finer discretization along the y direction was used in order to better model the spatial extent of the SMT load resistor. The feed probe was modeled employing a quasi-static approach that modifies the magnetic field circling the wire [6]. The feed source was modeled by a simple gap voltage source V_s with a 50-Ω source resistance incorporated into a single cell at the feed point. The magnetic fields circling the source were modeled in the same fashion as a thin wire to give the cross-section of the source specified physical dimensions [7]. A magnetic frill type source was also investigated, but yielded little improvement over the wide gap type source [8]. The resistor was modeled as a lumped element using a subcellular algorithm [9]. The width of the SMT is approximately that of the feed probe diameter and the physical cross-section dimensions were modeled with the same diameter as that of the feed probe by modifying the magnetic field components circling the SMT in the same fashion as for the source. The slot was modeled with a capacitive thin-slot subcellular algorithm to avoid a small mesh dimension [10], and perfectly-matched-layer (PML) absorbing boundary conditions were employed for the 3D simulations [11].

A sinusoidally modulated Gaussian pulse was employed as the excitation. The source voltage as a function of time t was

$$V_s(t) = e^{-\alpha^2(t-t_0)^2} cos[2\pi f_0(t - t_0)], \tag{2}$$

where $f_0 = \frac{f_{upper}+f_{lower}}{2}$ is the center frequency (f_{lower} is the starting frequency and f_{upper} is the stopping frequency), and α and t_0 are

$$\alpha = \frac{\pi(f_{upper} - f_{lower})}{\sqrt{-ln(b_{BW})}}, \tag{3}$$

$$t_0 = \frac{1}{\alpha}\sqrt{-ln(b_t)}, \tag{4}$$

where b_{BW} is the minimum pulse level which is unaffected by computational noise, and b_t is the maximum allowable

pulse level at $t = 0$. b_{BW} and b_t were 0.0001 and 0.001, respectively, so that the temporal pulse was greater than two orders of magnitude below the maximum at the beginning and end of the pulse. A time step of 8.3333 ps was used. The time-history of the voltage V_0 across the source and source impedance, and the current I_0 through the source were stored, and an FFT was employed to calculate frequency-domain quantities. A total of 20,000 time steps was required for a good resolution in the frequency domain. In simulations with frequency bands containing very high Q resonances, e.g., 1.36 GHz in Figure 4 (a) for the case without the lossy material, an additional 20,000 time steps, or 40,000 total were required in order for the stored energy to decay and minimize ringing. Prony's method has also been used to decrease the required time record [12]. The computed real power delivered by the source normalized to the source voltage was calculated as

$$P_{FDTD} = \frac{1}{2|V_s|^2} Re(\hat{V}_0 \times \hat{I}_0^*). \quad (5)$$

The maximum power available from the source was 2.5 mW.

The measured and simulated delivered power are shown in Figure 4 (a). In general, the agreement is good. The cavity modes TM_y101, TM_y111, and TM_y201 were excited at 0.88 GHz, 1.37 GHz, and 1.43 GHz, respectively, while resonances associated with the slot were excited at 1.12 GHz, 1.24 GHz, and 1.53 GHz. The calculated radiated power through the slot is also shown in Figure 4 (a). The power radiated at the half-wavelength slot resonance frequency 1.24 GHz was 44% of the available power, and 27% and 89% of the available power was radiated through the slot at 1.12 GHz and 1.53 GHz, respectively. The power radiated through the slot at the TM_y101, TM_y111, and TM_y102 cavity modes was 12%, 34%, and 32% of the available power, respectively. Significant power was radiated through the slot at the cavity resonance below the half-wavelength slot resonance.

The results of two-port radiated measurements are shown in Figure 4 (b). The frequency-match of resonances in $|S_{11}|$ and $|S_{21}|$ at cavity mode and slot resonances is shown by arrows. The $|S_{11}|$ is related to the delivered power by Equation (1), while the $|S_{21}|$ is related to the radiated power. Since the antenna factor was not included in the calibrations, only qualitative comparison can be made. However, it is clear that radiation at TM_y101 (0.88 GHz), TM_y111 (1.37 GHz), and TM_y201 (1.43 GHz) cavity mode resonances was significant in both the simulated and measured results.

Loss added to resonant structures typically reduces the Q of the resonances. In a radiating system, such as an enclosure with perforations, this principle can be potentially applied to reduce EMI. The effect of a lossy material in reducing EMI was investigated in the S-1000, both in the

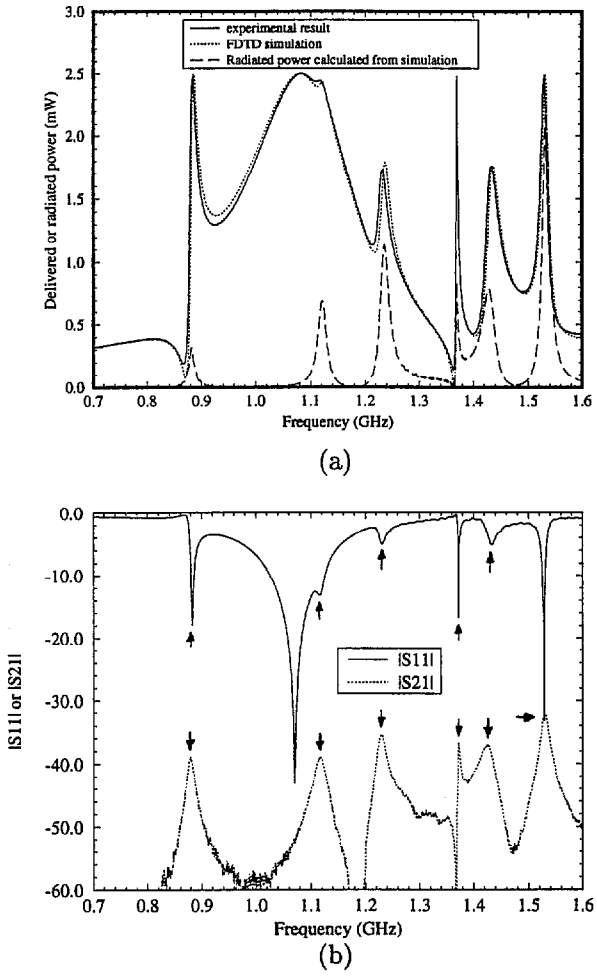

Figure 4. For the simple rectangular enclosure, (a) measured and simulated delivered power and the power radiated through the slot calculated from the FDTD simulation, and (b) measured $|S_{11}|$ and $|S_{21}|$, for the simple rectangular enclosure.

functioning hardware, and with swept frequency measurements. Loss was introduced in the enclosure by adhering the lossy material to the interior top, bottom, and back faces, as well as the center plane. For the same patch source at Point A, $|S_{21}|$ measurements with and without a lossy material are shown in Figure 5. The background noise with all apertures sealed is also shown. The effect of the lossy materials was significant for both $|S_{21}|$ and $|S_{11}|$ at frequencies above 600 MHz. The radiation decreased for most of the resonances. The decrease in radiation ($|S_{21}|$) is approximately 10 dB, 6 dB, 6 dB, and 7 dB for cavity modes at 1.01 GHz, 1.04 GHz, 1.38 GHz, and 1.89 GHz, respectively. Employing lossy materials inside a working S-1000 system also showed a similar effect. At frequencies above 500 MHz, the decrease in radiated EMI was greater than 10 dB for most CPU harmonics, while at frequencies

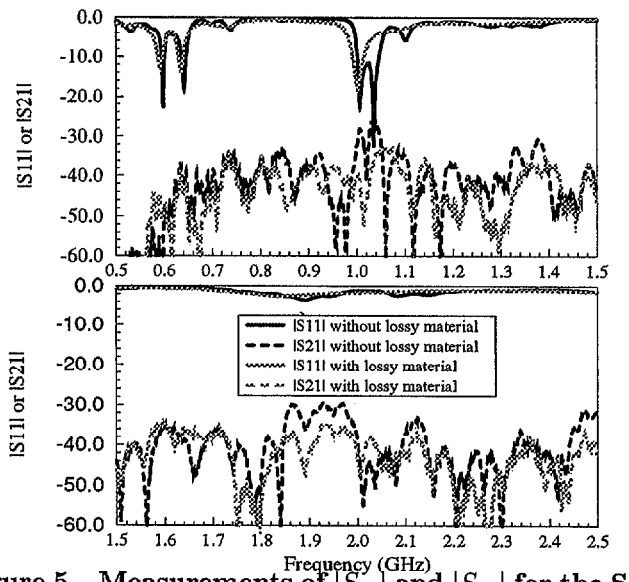

Figure 5. Measurements of $|S_{11}|$ and $|S_{21}|$ for the S-1000 excited by patch source at Point A, with and without lossy materials.

below 500 MHz, the effect was not significant.

III. Summary and Conclusion

Radiation through slots and apertures in shielding enclosures at cavity mode resonances was investigated in an S-1000 server enclosure and a simple rectangular cavity. Two-port S-parameter measurements showed that significant radiation through slots and apertures occurred at enclosure cavity resonances. FDTD simulations for the simple rectangular enclosure agreed with the measurements, and the results indicated that significant power was radiated through slots at cavity mode resonances. The potential of a lossy material in reducing EMI was also demonstrated in the S-1000 enclosure. However, further work is necessary in understanding the coupling mechanisms, investigating the effect of interior electronics, and determing the optimal way of applying loss in the enclosure. The agreement between the simulated and measured results for the simple cavity indicated that these issues can be explored relying on FDTD simulations, with fewer, more selective experiments for corroboration.

References

[1] H. Moheb, L. Shafai and J. Shaker, "Numerical solution of radiation from single and multiple arbitrary apertures backed by a cavity", *IEEE Antennas and Propagat. Symposium, 1992 Digest*, vol. 1, pp. 61-64, 1992.

[2] S. Daijavad and B. J. Rubin, "Modeling common-mode radiation of 3D structures", *IEEE Trans. Electromagn. Compat.*, vol. 34, pp. 57-61, February 1992.

[3] C. A. Balanis, *Advanced Engineering Electromagnetics;* John Wiley & Sons; New York, 1989.

[4] R. B. Collin, *Foundations for Microwave Engineering.* McGraw-Hill; 1992.

[5] S. Radu, M. Li, D. M. Hockanson, Y. Ji, J. Nuebel, J. L. Drewniak, T. H. Hubing, and T. P. VanDoren, "The Effect of Internal Compartmentalization of Metallic Enclosures for Reducing EMI", submitted to *IEEE Trans. Electromagn. Compat. Symp.*, 1997.

[6] A. Taflove, *Computational Electrodynamics.* Artech House; Boston, 1995.

[7] David M. Hockanson, James L. Drewinak, Todd H. Hubing and Thomas P. Van Doren, "FDTD modeling of common-mode radiation from cables," *IEEE Trans. Electromagn. Compat.*, vol. 38, pp. 376-387, August 1996.

[8] M. Li, *Investigation of Electromagnetic Interference Through Slots in Shielding Enclosures: Finite-Difference Time-Domain Simulations and Experiments*, M. S. Thesis, University of Missouri-Rolla, 1996.

[9] Yuh-Sheng Tsuei, A. C. Cangellaris and J. L. Prince, "Rigorous electromagnetic modeling of chip-to-package (first-level) interconnections," *IEEE Transactions on Components, Hybrids, and Manufacturing Technology,* vol. 16, pp.876-882, December 1993.

[10] J. Gilbert and R. Holland, "Implementation of the thin-slot formalism in the finite-difference EMP code THREDII," *IEEE Trans. Nuclear Sci.*, vol. NS-28, pp. 4269-4274, December 1981.

[11] J. P. Berenger, "Perfectly matched layer for the absorption of electromagnetic waves," *Journal of Computational Physics*, vol. 114, pp. 185-200, October 1994.

[12] W. L. Ko and R. Mittra, "A comparison of FD-TD and Prony's methods for analyzing microwave integrated circuits", *IEEE Trans. Microw. Theory Tech.*, vol. 39, pp. 2176-2181, December 1991.